Deposited via The University of Sheffield.

White Rose Research Online URL for this paper:
https://eprints.whiterose.ac.uk/id/eprint/100755/

Version: Accepted Version

Predicting railway wheel wear under uncertainty of wear coefficient, using universal kriging

Marzia A. Cremona[a,b,*], Binbin Liu[c], Yang Hu[d], Stefano Bruni[c], Roger Lewis[e]

[a]*MOX - Department of Mathematics, Politecnico di Milano, Italy*
[b]*Present address: Department of Statistics, Penn State University, University Park, USA*
[c]*Department of Mechanical Engineering, Politecnico di Milano, Italy*
[d]*Department of Energy, Politecnico di Milano, Italy*
[e]*Department of Mechanical Engineering, The University of Sheffield, Sheffield, UK*

Abstract

Railway wheel wear prediction is essential for reliability and optimal maintenance strategies of railway systems. Indeed, an accurate wear prediction can have both economic and safety implications. In this paper we propose a novel methodology, based on Archard's equation and a local contact model, to forecast the volume of material worn and the corresponding wheel Remaining Useful Life (RUL). A universal kriging estimate of the wear coefficient is embedded in our method. Exploiting the dependence of wear coefficient measurements with similar contact pressure and sliding speed, we construct a continuous wear coefficient map that proves to be more informative than the ones currently available in the literature. Moreover, this approach leads to an uncertainty analysis on the wear coefficient. As a consequence, we are able to construct wear prediction intervals that provide reasonable guidelines in practice.

Keywords: Wear Prediction, Wear Coefficient, Universal Kriging, Remaining Useful Life

1. INTRODUCTION

In the maintenance of railway wheel suspending operations, reductions in transportation and safety accidents caused by unforeseen failures are very costly, both in terms of repairs and unrealized profits. These huge losses arouse great interest in the development of efficient methods and procedures that could reduce unforeseen failures and improve equipments safety and availability [1]. Prognostics enables safer and more reliable operations, allowing the equipment to run as long as it is healthy. Moreover, it is useful for optimally scheduling the maintenance interventions. In other words, prognostics substantially helps in achieving the goals of maximum safety and availability, minimum unscheduled shutdowns of transportation and economic maintenance [2], which are issues of utmost relevance for railway systems. In this paper, we propose a novel methodology to predict the future degradation of railway wheel, by means of wear, and to calculate the Remaining Useful Life (RUL), namely the residual distance that the wheel can run according to its design specifications.

According to [3], the wheel wear of rail vehicles is typically predicted evaluating either the sliding contact by using Archard's equation, or rolling/sliding contact by using the energy dissipation effect (developed for the first time in [4]). Archard's equation is more commonly used in railway industry for wear prediction [3, 5, 6, 7]; indeed, it has been successfully applied in [8] to predict wear of roller bearings, which is quite similar to wheel-rail rolling contact wear. For this reason, we choose to employ Archard's equation in our methodology. Briefly, Archard's equation states that the volume of material worn V_w is proportional to the sliding distance s and the normal load N, and inversely proportional to the hardness of material H, namely

$$V_w = K\frac{sN}{H}, \tag{1}$$

where the wear coefficient K is a dimensionless constant that indicates the severity of wear.

Wear is a complicated process that involves a large variety of contributions from different phenomena, combining the short-term dynamics that produces the wear debris and the long-term dynamics of the material transportation that goes on. For these reasons, exact wear prediction is usually unattainable. As for engineering applications, the sliding contact model seems sufficiently accurate and adequate to approximate the wheel failure due to wear.

The wear coefficient K plays an important role in wheel wear prediction through equation (1). Currently, it can be derived from laboratory tests or, alternatively, from extensive calibrations based on geometrical comparisons between simulated and measured wheel profiles. Nowadays there exist in literature a few wear charts and maps for the wear coefficient K as a function of contact pressure p and sliding speed v, concerning different rail-wheel materials and environments (see for example Figure 1, with data from [5], or the charts presented in

*Corresponding author
Email addresses:* `mac78@psu.edu` (Marzia A. Cremona),
`binbin.liu@polimi.it` (Binbin Liu), `yang.hu@polimi.it` (Yang Hu),
`stefano.bruni@polimi.it` (Stefano Bruni),
`roger.lewis@sheffield.ac.uk` (Roger Lewis)

[9]). Conversely, there are really limited data on cases where third body materials (grease, water, friction modifiers etc.) are present [10]. The available wear maps are mostly for dry conditions. Furthermore, they are not very accurate due to the limited number of experiments available in each condition. Hence such charts are of restricted usefulness and it would be desirable to have more accurate maps.

Given this background, it is advisable to provide a measure of the uncertainty concerning wear prediction. Actually, no uncertainty analysis is usually supplied by available wear prediction tools. In sensitivity analysis, metamodels are built to approximate the behavior of large computational models and study how the inputs can influence the predicted output values. Several global sensitivity analysis techniques have been investigated in literature (see e.g. [11]). Regression-based methods employ linear regression models to measure the effect of the inputs on the model response. For example, polynomial chaos expansion [12, 13] and sparse polynomial chaos expansion [14] of the response have been shown to provide an efficient and accurate computation of global sensitive indices. Another class of techniques is based on an ANOVA decomposition (variance-based methods) of the output variance as a sum of contribution of the different inputs. In this framework, a complex model can be approximated via smoothing spline ANOVA [15] or using state dependent parameter modeling [16, 17, 18]. Gaussian process models [19] and kriging [20] have also been successfully applied to build metamodels. All these different approaches are very useful when there is uncertainty about the input values in a particular setting and evaluating the actual model response on all possible input configurations requires too much time. An underlying hypothesis is the smoothness of the function of response given inputs. Here we want to employ a methodology similar to these global sensitivity analysis techniques, to compute the wear coefficient K given the contact pressure p and sliding speed v as inputs. In this setting we do not have any uncertainty about the values of pressure and speed (since they are derived by the local contact model as explained in Section 2). However, an approximate model of the wear coefficient K is needed because, as noted above, only a limited number of experiments, for particular choices of p and v, are available.

In this paper we propose a novel wear prediction methodology that provides an assessment for the wear of a rail vehicle wheel with uncertainty. The wear coefficient is estimated in a continuous way by using spatial statistic techniques (in particular, universal kriging). In this way, we are able to take advantage of the spatial dependence of measures (in the v and p plane) to overcome the issue of having few available data. In addition, these techniques provide a measure of the uncertainty concerning the value of the coefficient K. Hence, we can compute a prediction interval for K associated to each choice of v and p instead of a single point prediction. As a consequence, our model predicts a range for the amount of wheel material removal and a prediction interval for the RUL.

In the following, Section 2 contains the wheel wear model proposed; Section 3 shows the mathematical model used to estimate K with uncertainty, and Section 4 describes the prediction of RUL. Finally, applications of the proposed methodology are presented in Section 5.

2. WHEEL WEAR MODEL

The degradation model for wheel wear prediction adopted in this article is shown in Figure 2. We consider the wear coefficient K involved in Archard's equation as a function of contact pressure p and sliding speed v, both varying over the specific contact patch of interest. A local contact model is implemented by employing the non-Hertzian contact method developed in [21]. Using this method, we estimate the shape of the contact patch and the pressure distribution given the normal force, the local geometry and the material properties. Here the contact stress distribution is assumed to be ellipsoidal and it is discretized in the direction of rolling. The density of discretization can be tuned to ensure that the size of each cell is small enough to consider the pressure p as a constant on the cell. Next, the corresponding sliding speed for each cell in the slip area of the contact patch is obtained using the method suggested in [5], as depicted in Figure 3. In detail, the sliding velocity is given by

$$\vec{v} = V_{vehicle} \left[\begin{array}{c} \gamma_2 + \gamma_3 x \\ \gamma_1 - \gamma_3 y \end{array} \right], \qquad (2)$$

where $V_{vehicle}$ is is the forward speed of wheel; γ_1, γ_2 and γ_3 are respectively the longitudinal, lateral and spin creepages; x, y are the Cartesian coordinates of the contact patch. The creepages can be obtained from multibody system (MBS) simulation of a rail vehicle or, alternatively, from field measurement combined with some post-processing. We employ the latter strategy in our methodology, in accordance with [3]. By using Archard's equation (1), the wear volume at the center of each cell j is therefore approximated by

$$V_{w,j} = K(p_j, v_j) \frac{s_j N_j}{H} \qquad j = 1, \ldots, n. \qquad (3)$$

Then, we compute the total wear volume after a given running distance of the wheel, assuming that the contact patch remains constant when the wheel is running on a straight track, using the formula

$$V_{w,tot} = V_{w,patch} \left(1 + m \frac{L}{2a} \right), \qquad (4)$$

where $V_{w,patch} = \sum_{j=1}^{n} V_{w,j}$ is the wear volume over the contact patch, m is the maximum discrete number of contact patches in the rolling direction, L is the running distance of the wheel center of mass, and $2a$ is the maximum length of the contact patch in the rolling direction (see Figure 4).

3. WEAR COEFFICIENT ESTIMATION WITH UNCERTAINTY

To estimate (with uncertainty) the wear coefficient K that is needed in the wheel wear model presented in Section 2, we use data taken from [22] as collected and preprocessed by Lewis and Olofsson in [9]. Experiments have been carried out using
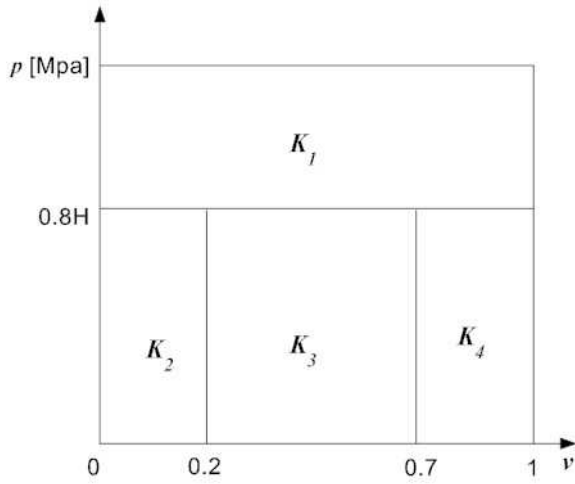
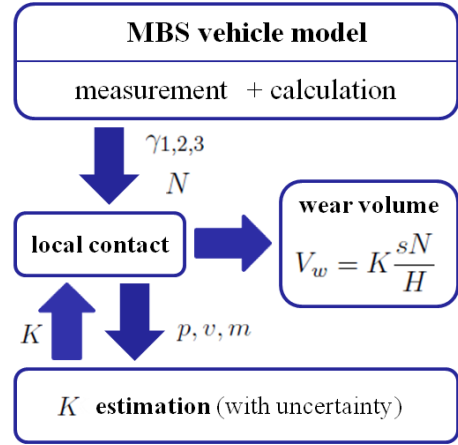Figure 1: Wear coefficient K chart, with data from [5].

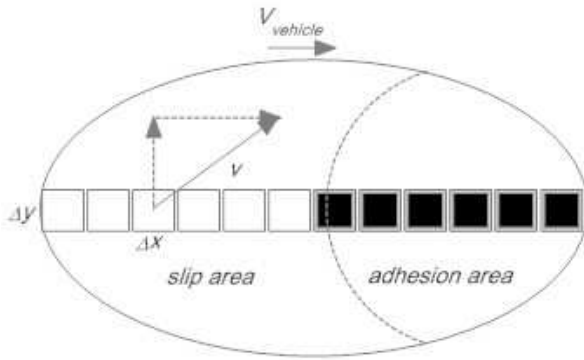Figure 2: The proposed methodology for wheel wear prediction.

Figure 3: Sliding speed for each cell in contact patch, computed as suggested in [5].
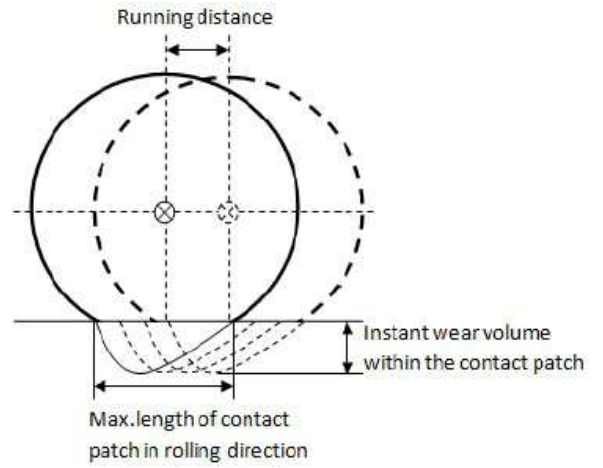

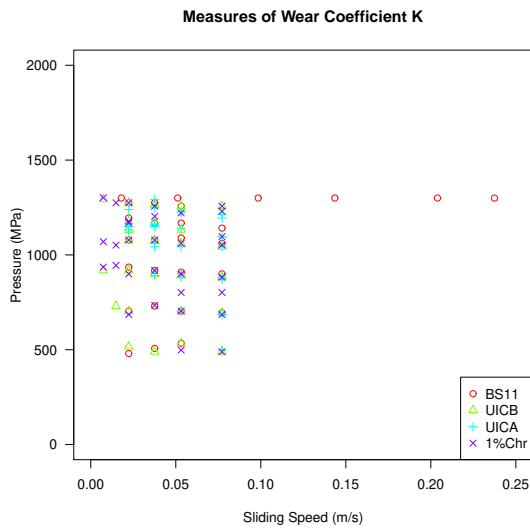Figure 4: Illustration of the total wear volume calculation in (4).

Figure 5: Locations of wear coefficient K measures. Colors indicate the different rail disc materials.

	Estimate	Std. Error	t value	$Pr(> |t|)$
β_0	2.564	0.114	22.52	<2e-16
β_1	-3.651	0.442	-8.26	6.17e-13
β_2	-3.081	0.514	-5.99	3.33e-08
β_3	-4.145	0.571	-7.27	8.31e-11
β_4	14.534	2.213	6.57	2.33e-09
β_5	22.564	5.079	4.44	2.30e-05
β_6	23.498	4.337	5.42	4.16e-07
β_7	0.00243	0.000431	5.64	1.57e-07
β_8	0.00170	0.000433	3.91	1.67e-04
β_9	0.00258	0.000470	5.49	3.10e-07

Table 1: Estimates, standard errors and t-tests for the nullity of the coefficients of the linear model in (8).

a wear testing machine in dry, cool condition for Class D tyre and four different rail materials: BS11, UICA, UICB and 1% Chrome. We have more than 100 measurements of the wear coefficient, according to varying sliding speed v and contact pressure p. Figure 5 shows the locations of wear coefficient K measurements, colored according to the rail material used. Unfortunately, most of observations lie in the range 400-1300 MPa and 0.00-0.08 m/s and only few experiments belong to more extreme regimes. Moreover, the distribution of the measurements in the v and p plane differs among the different rail materials. In particular, all the extreme regimes measurements belong to BS11 rail. Therefore, we propose to estimate the wear coefficient K with a spatial statistics model (universal kriging), exploiting similarities among different materials and the spatial dependence of data (in the v and p plane). In this way we are able to partially overcome the limitation of having few available measurements. In the following, we briefly review the fundamentals of universal kriging, as employed here. A detailed presentation of spatial statistics theory can be found, for instance, in [23].

Let $D \subset \mathbb{R}^2$ be a fixed subset of $\mathbb{R}^2$ that contains a rectangle of positive area, and consider the random process $\{Z(\mathbf{s}) : \mathbf{s} \in D\}$. Given a set of N realizations $Z(\mathbf{s}_1), \dots, Z(\mathbf{s}_N)$ at known spatial locations $\{\mathbf{s}_1, \dots, \mathbf{s}_N\}$, we are interested in finding the random process Z that best describes the observed data. In universal kriging, the assumed model is

$$Z(\mathbf{s}) = \mu(\mathbf{s}) + \delta(\mathbf{s}), \quad \mathbf{s} \in D \quad (5)$$

where $\mu(\cdot) = \beta_0 f_0(\cdot) + \cdots + \beta_p f_p(\cdot)$ is the drift (or large scale variability) given by an unknown linear combination of known functions, and $\delta(\cdot)$ is a zero-mean second-order stationary and isotropic random process, i.e. for every $\mathbf{s}, \mathbf{s}_i, \mathbf{s}_j \in D$ we have $E[Z(\mathbf{s})] = \mu(\mathbf{s})$, $E[\delta(\mathbf{s})] = 0$ and $Cov(\delta(\mathbf{s}_i), \delta(\mathbf{s}_j)) = C(\|\mathbf{s}_i - \mathbf{s}_j\|)$. Given these assumption, the random process has variogram $2\gamma(\cdot)$, defined by $2\gamma(\mathbf{s}_i - \mathbf{s}_j) = Var(\delta(\mathbf{s}_i) - \delta(\mathbf{s}_j))$. The universal kriging prediction in a new location $\mathbf{s}_0$ is then given by the best linear unbiased predictor of the form

$$\hat{Z}(\mathbf{s}_0) = \sum_{i=1}^{N} \lambda_i Z(\mathbf{s}_i). \quad (6)$$

Using the kriging prediction $\hat{Z}(\mathbf{s}_0)$ and the corresponding variance $\hat{\sigma}^2(\mathbf{s}_0)$, prediction intervals can be constructed. Specifically, under the assumption that Z is Gaussian, the interval

$$I(\mathbf{s}_0) = \left(\hat{Z}(\mathbf{s}_0) - z_{1-\frac{\alpha}{2}} \hat{\sigma}(\mathbf{s}_0), \hat{Z}(\mathbf{s}_0) + z_{1-\frac{\alpha}{2}} \hat{\sigma}(\mathbf{s}_0)\right) \quad (7)$$

where $z_{1-\frac{\alpha}{2}}$ is the quantile of order $1 - \frac{\alpha}{2}$ of the standard normal distribution, is the $(1-\alpha)100\%$ prediction interval for $\hat{Z}(\mathbf{s}_0)$, i.e. the interval such that $Pr(Z(\mathbf{s}_0) \in I(\mathbf{s}_0)) = (1-\alpha)100\%$.

3.1. A linear model for the drift

The first step consists of using a linear model to estimate the drift (large scale variability) and to assess whether there are statistically significant differences in wear coefficient among the four different rail materials (details on this type of model can

be found, for example, in [24]). Given that the distribution of K is highly asymmetrical and concentrated on very small values, we perform a logarithmic transformation on this variable. Then we start fitting a linear model with response $\log(K)$, in which sliding speed v and contact pressure p constitute the quantitative predictors, and rail materials make up categorical variables. Interactions between sliding speed and rail materials, as well as between contact pressure and rail materials, are also included in the complete linear model. Stepwise variable selection leads to the reduced model:

$$\begin{aligned} \log(K) = \ &\beta_0 + \beta_1 \cdot BS11 + \beta_2 \cdot UICB + \beta_3 \cdot 1\%Chr \\ &+ \beta_4 \cdot BS11 \cdot v + \beta_5 \cdot UICB \cdot v + \beta_6 \cdot 1\%Chr \cdot v \\ &+ \beta_7 \cdot BS11 \cdot p + \beta_8 \cdot UICB \cdot p + \beta_9 \cdot 1\%Chr \cdot p + \epsilon, \end{aligned}$$
$$(8)$$

where $BS11$, $UICB$ and $1\%Chr$ are dummy variables that take the value 1 to indicate the corresponding rail material (we have $UICA$ when all the three dummy variables are 0). Table 1 shows coefficients estimates, standard errors and p-values of the t-tests assessing whether such coefficients are 0: all the regressors are significant. Moreover, the F-test assesses the significance of the model (p-value $< 2.2e - 16$) and the adjusted coefficient of determination R^2 is quite high (0.65), so the model fits the data quite well. However, residuals do not respect the independence assumption, that is fundamental for the linear model. In fact, as revealed for example by the sample variogram in Figure 6, residuals are spatially correlated (the space being the v and p plane); hence, we exploit this feature to accurately predict the value of the coefficient K by using universal kriging, as explained below. Figure 7(a) shows the drift given by the linear model, concerning BS11 rail. The drift for the other rail materials can be found in panel (a) of the Additional Figures A.11, A.12 and A.13.
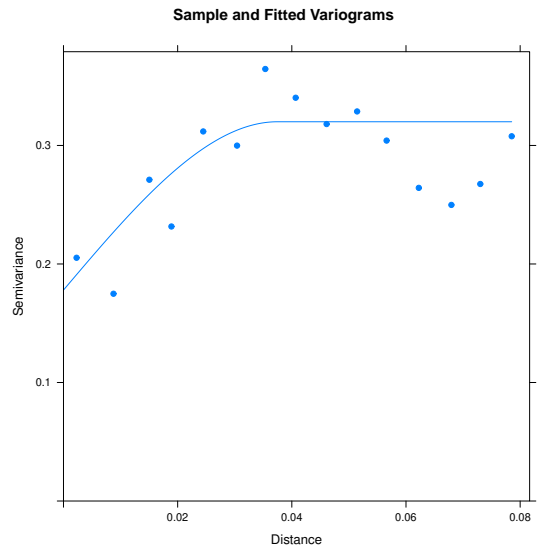

Figure 6: Sample variogram (dots) and fitted spherical variogram (line).
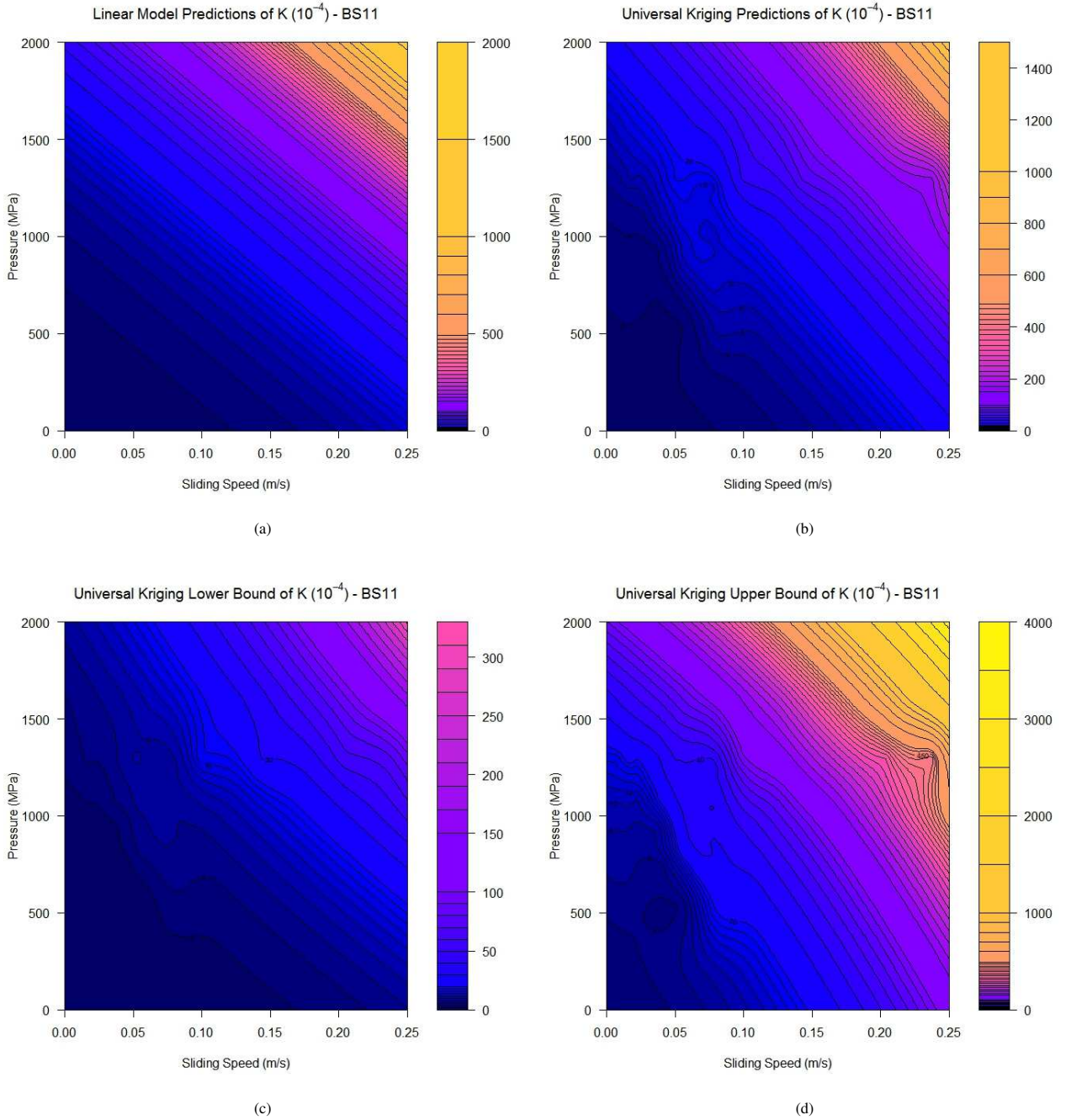
4

Figure 7: Wear coefficient K (10^{-4}) maps concerning BS11 rail discs: (a) describes the drift given by the linear model (large scale variability); (b) is the prediction with universal kriging; (c) and (d) show the 90% pointwise prediction intervals.

3.2. Prediction and uncertainty analysis with universal kriging

We consider our data as spatial data, with coordinates given by the sliding speed v (m/s) and the contact pressure $\tilde{p}$ (10^{-4} MPa), where the pressure scale is changed in order to obtain comparable coordinates ranges. Our aim is to predict the wear coefficient K within the domain $D = \{0 < v < 0.25, \ 0 < \tilde{p} < 0.2\}$, taking advantage of the spatial correlation of data. We adopt model (5) with random process $Z(\cdot) = \log(K(\cdot))$, i.e.

$$\log(K(\mathbf{s})) = \mu(\mathbf{s}) + \delta(\mathbf{s}), \quad \mathbf{s} \in D, \tag{9}$$

where the large scale variability $\mu(\cdot)$ is chosen as the reduced linear combination of the regression model (8) obtained above. We fit a spherical variogram model to the estimated one, fixing the nugget thanks to some repeated measures of the wear coefficient in the same position $\mathbf{s}$ (see Figure 6). The isotropic variogram is given by

$$\gamma(\mathbf{h}) = \begin{cases} 0 & \mathbf{h} = \mathbf{0} \\ c_0 + c_s \left[\frac{3\|\mathbf{h}\|}{2a_s} - \frac{1}{2} \left(\frac{\|\mathbf{h}\|}{a_s} \right)^3 \right] & 0 < \|\mathbf{h}\| \le a_s \\ c_0 + c_s & \|\mathbf{h}\| > a_s \end{cases} \tag{10}$$
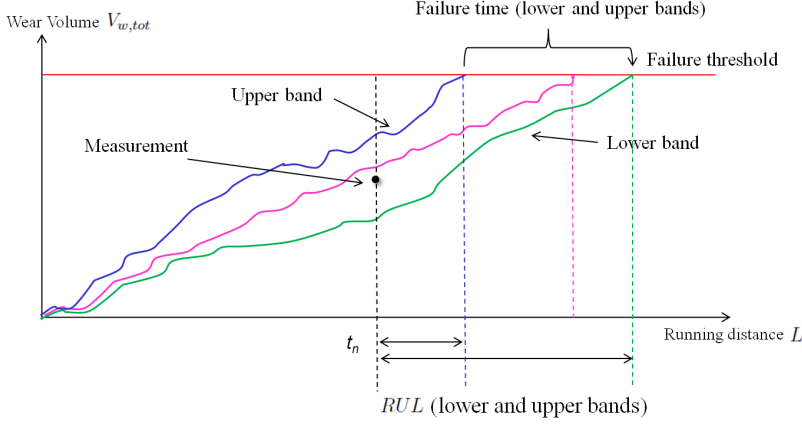
5

Figure 8: Sketch map of RUL prediction.

	Large creepage	Small creepage
Longitudinal creepage γ_1	-0.0020	-0.0004
Lateral creepage γ_2	-0.0015	-0.0003
Normal force N	60 kN	
Velocity $V_{vehicle}$	30 m/s	

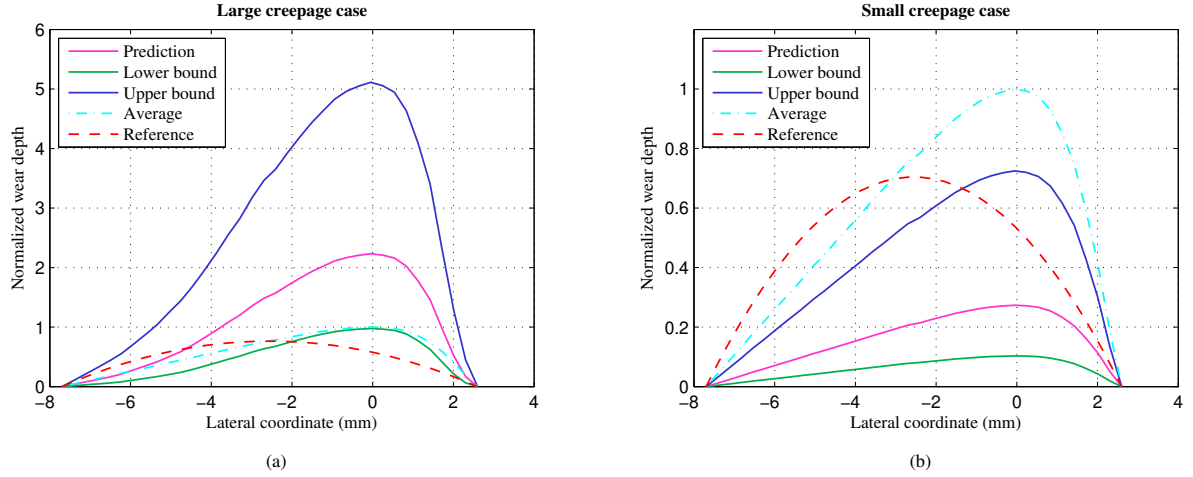Table 2: Parameters used in the two conditions considered.

Figure 9: Wear distribution over contact patch in (a) large creepage case and (b) small creepage condition. The different lines refer to the values of the wear coefficient K used: universal kiging predictions (Prediction), 90% prediction intervals (Lower bound and Upper bound), average values in each region of the wear chart in Figure 1 (Average) and constant K from [3] (Reference).

where the nugget is $c_0 = 0.178$, the parameter of the spherical model is $c_s = 0.142$ and the range is $a_s = 0.0375$. Universal kriging is then used to predict $\log(K(\cdot))$ on a grid in the domain D, for each of the four rail materials considered. The prediction variance is also computed on the grid, allowing the construction of 90% pointwise prediction intervals for $\log(K(\cdot))$ by equation (7) with $\alpha = 0.1$ on each point of the grid, under the assumption that $\log(K(\cdot))$ is Gaussian (and hence $K(\cdot)$ is log-normal). Figure 7(b) shows the prediction obtained with this model concerning the BS11 rail material, while Figures 7(c) and (d) depict the 90% pointwise prediction intervals. Analogous plots for the other rail materials can be found in Additional Figures A.11, A.12 and A.13. It is important to notice that kriging prediction is much more informative than the piecewise constant chart in Figure 1 from [5]. Moreover, it is comparable to the wear coefficient map in [9] and, in addition, it is associated with a rigorous quantification of uncertainty (prediction intervals).

4. REMAINING USEFUL LIFE PREDICTION

We use a model-based prognostics approach to predict the RUL of train wheel (reviews on model-based prognostics approaches for RUL computation can be found in [25] and [26]). First we use Archard's equation (1) and the wear model presented in Section 2 to predict the wheel degradation trend in the future. Next, we combine this prediction with a known failure threshold to calculate the RUL (see [27] and [28]). The RUL predicted at $L(i)$ (i.e. for a wheel that has already run a distance $L(i)$) is given by the expression

$$\text{RUL}(L(i)) = \left[L_f(i) \mid V_{w,tot}\left(L_f(i)\right) = V_T \right] - L(i), \quad (11)$$

where $L_f(i)$ is the predicted running distance when the wear of the wheel reaches its failure threshold V_T. $L_f(i)$ can be obtained using (4). In our application, the only source of uncertainty in $RUL(L(i))$ is the wear coefficient K. Using the upper and lower bounds of the 90% pointwise prediction intervals for

6

	$V_{w,tot,L}$ ($\times 10^3$ mm^3)	$V_{w,tot,P}$ ($\times 10^3$ mm^3)	$V_{w,tot,U}$ ($\times 10^3$ mm^3)	Factor	RUL_L ($\times 10^3$ km)	RUL_P ($\times 10^3$ km)	RUL_U ($\times 10^3$ Km)
Case 1	58.02	130.29	292.84	0.5525			
Case 2	104.92	243.39	565.85	1.0320	326.61	112.74	20.40
Case 3	66.44	151.63	346.52	0.6429			
		(a)				(b)	

Table 4: Simulation results concerning (a) the wear volume in the three cases of contact locations and (b) the RUL in the second case. $V_{w,tot,L}$, $V_{w,tot,P}$ and $V_{w,tot,U}$ indicate, respectively, the total wear volume obtained by applying the lower bound, the prediction and the upper bound of the wear coefficient K estimated through universal kriging. RUL_L, RUL_P, RUL_U have the same meaning for the RUL.

K computed in Section 3, we can create inferior and superior bands for RUL can be predicted. Figure 8 shows the sketch map of RUL prediction.

5. SIMULATION RESULTS

5.1. The effect of wear coefficient K on wear prediction

In order to analyze the effect of the wear coefficient K on wear prediction over a single contact patch, two typical conditions are considered for comparison: large creepage and small creepage (details about the parameters used in the two conditions can be found in Table 2). In both cases the wheel/rail combination is chosen so that the wheel profile is S1002 and the rail profile is UIC60, with the material property of BS11 and an inclination of 1/20 for each rail. The normal force N is 60 kN and the speed $V_{vehicle}$ is 30 m/s.

Simulations are carried out using the universal kriging predictions and the 90% prediction intervals for the wear coefficient K as computed in Section 3 (Figure 7). Moreover, we compare our methodology with simulations performed evaluating the wear coefficient K in different ways. In particular, we simulate the wear volume considering average values in each region of the wear chart in Figure 1 (data from [5]) and assuming the coefficient K is constant, with value 3.56×10^{-4} according to reference [3]. The resulting wear depths have been normalized with respect to the maximum value obtained in the average K case. Figure 9 depicts the wear distribution over a contact patch with the given conditions, for the different choices of the wear coefficient.

These results suggest that uncertainty in the wear coefficient affects both the wear distribution and the wear amount over the whole contact patch, depending on the contact situation. The constant and average K lead to underestimating and overestimating the wear volume with respect to the prediction band obtained using universal kriging, in simulation scenarios of large and small creepages, respectively.

5.2. Application to a real case prediction

One real case is chosen from the literature with the aim to validate our methodology. According to [3], we use the parameters shown in Table 3 for the simulation. In addition, the wheel/rail contact combination is chosen to be S1002 wheel profile and UIC60 rail profile as in [3], with rail material BS11. We consider three contact locations around the nominal rolling circle of the wheel from left to right, because the exact contact position is not provided in the reference. As for the computation of the RUL, we fix the failure threshold at 800×10^3 mm^3, corresponding to a re-profile interval of the wheel. This threshold is used here as example and should not be adopted in practice: in fact, in each real application the threshold should be carefully chosen based on specific circumstances.

The results obtained using our methodology to compute wear volume are given in Table 4(a), and the corresponding RUL in case 2 in Table 4(b). Moreover, the wear distributions over the contact patch in the second case are presented in Figure 10. We can observe that the choice of wear coefficient influences the distribution of wear depth over the contact patch and, consequently, affects the vehicle dynamic behavior.

Comparing simulation results with the measured wear volume (235.84×10^3 mm^3), we see that our prediction factors, defined as the ratio between calculated and measured values, range from 0.55 to 1.03 in the three different contact locations considered. In all cases, these results are much better than by fixing $K = 3.56 \times 10^{-4}$ as in [3], which leads to a prediction factor of 4.23. Moreover the measured data falls, in each of the three contact locations, inside our prediction interval. Hence, we can conclude that our prediction methodology is quite effective.

6. CONCLUSIONS

In this paper we proposed a novel wear prediction methodology that accounts for dependence of wear coefficient K on

Longitudinal creepage γ_1	0.00043	Normal force N	63.396 kN
Lateral creepage γ_2	0.00156	Running distance L	49300 km
Spin creepage γ_3	0.163 1/m	Constant wear coefficient K	3.56×10^{-4}
Velocity $V_{vehicle}$	27.8 m/s	Measured wear volume	235.84×10^3 mm^3

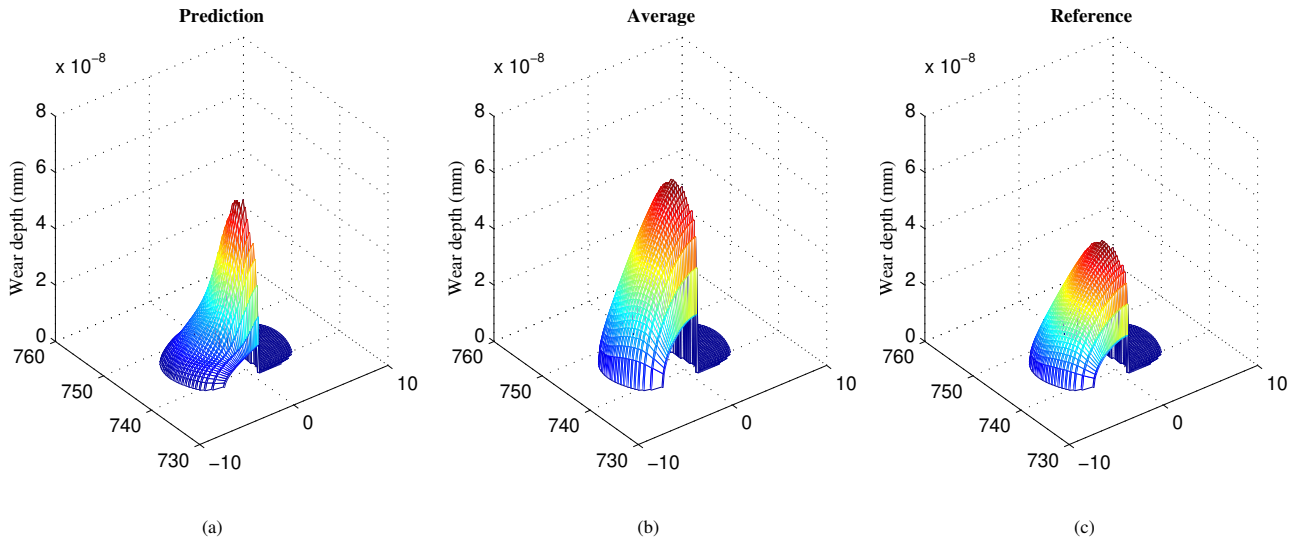Table 3: Relevant parameters for the simulation, from [3].

Figure 10: Wear distribution over contact patch simulated by using (a) universal kriging prediction for *K*, (b) average *K* values in each region of the wear chart in Figure 1 and (c) constant *K* from [3].

contact pressure and sliding speed, as they vary over the contact patch. Our methodology also quantifies uncertainty on *K*.

We applied this approach to two typical contact conditions in Section 5.1, to analyze the effect of wear coefficient uncertainty on wear prediction over a single contact patch. The simulations revealed that both wear distribution and wear amount over the whole contact patch are affected by this uncertainty. This should be taken into account in wear prediction, especially when incorporating multibody dynamics simulation of rail vehicle system in the model.

In Section 5.2, we validated our methodology on a real case prediction. Our results are much better than those currently available in literature, and the measured wear volume falls inside our prediction intervals.

It should be noted that many factors involved in the prediction, such as material hardness, contact situation, creepages etc, are not known with accuracy and can affect final results, by adding errors. However, the uncertainty analysis we performed on the wear coefficient is expected account for these additional error sources. Therefore, the methodology proposed in this paper can provide reasonable guidelines in practice. Nevertheless, further studies on the effect of the uncertainty of the wear coefficient on wheel profile wear prediction are needed, as well as a strong validation of our methodology. Moreover, the method from [21] for the local contact model and the online calculation of wear coefficient enable our wear prediction model to be incorporated into multibody dynamics simulation (see [29]). This co-simulation technology is expected to be even more effective.

References

[1] J. Pombo, H. Desprets, R. Verardi, J. Ambrsio, M. Pereira, C. Ariaudo, N. Kuka, Wheel wear evolution and its influence on the dynamic behaviour of railway vehicles, in: 7th EUROMECH Solid Mechanics Conference, 2009.

[2] E. Zio, Prognostics and health management of industrial equipment, in: Diagnostics and Prognostics of Engineering Systems: Methods and Techniques, 2012, pp. 333–356. doi:10.4018/978-1-4666-2095-7.ch017.

[3] A. Asadi, M. Brown, Rail vehicle wheel wear prediction: a comparison between analytical and experimental approaches, Vehicle System Dynamics 46 (6) (2008) 541–549. doi:10.1080/00423110701589430.

[4] J. Elkins, B. Eickhoff, Advances in non-linear wheel rail prediction methods and their validation, Journal of Dynamic Systems, Measurement, and Control 104 (2) (1982) 133–142. doi:10.1115/1.3139688.

[5] T. Jendel, Prediction of wheel profile wear - comparisons with field measurements, Wear 253 (1-2) (2002) 89–99. doi:10.1016/S0043-1648(02)00087-X.

[6] A. Bevan, P. Molyneux-Berry, B. Eickhoff, M. Burstow, Development and validation of a wheel wear and rolling contact fatigue damage model, Wear 307 (1-2) (2013) 100–111. doi:10.1016/j.wear.2013.08.004.

[7] R. Enblom, On simulation of uniform wear and profile evolution in the wheel-rail contact, Ph.D. thesis, Royal Istitute of Technology (2006).

[8] U. Olofsson, S. Andersson, S. Bjorklund, Simulation of mild wear in boundary lubricated roller thrust bearings, in: AUSTRIB 98, Tribology at Work: Proceedings of the 5th International Tribology Conference, 1998. doi:10.1016/S0043-1648(00)00373-2.

[9] R. Lewis, U. Olofsson, Mapping rail wear regimes and transitions, Wear 257 (7-8) (2004) 721–729. doi:10.1016/j.wear.2004.03.019.

[10] Y. Zhu, J. Sundh, U. Olofsson, A tribological view of wheel-rail wear maps, International Journal of Railway Technology 2 (3) (2013) 79–91. doi:10.4203/ijrt.2.3.4.

[11] A. Saltelli, K. Chan, E. M. Scott, Sensitivity analysis, Vol. 1, Wiley New York, 2000.

[12] B. Sudret, Global sensitivity analysis using polynomial chaos expansions, Reliability Engineering and System Safety 93 (7) (2008) 964–979. doi:doi:10.1016/j.ress.2007.04.002.

[13] Y. Caniou, B. Sudret, Distribution-based global sensitivity analysis using polynomial chaos expansions, Procedia - Social and Behavioral Sciences 2 (6) (2010) 7625–7626. doi:doi:10.1016/j.sbspro.2010.05.149.

[14] G. Blatman, B. Sudret, Efficient computation of global sensitivity indices using sparse polynomial chaos expansions, Reliability Engineering and System Safety 95 (11) (2010) 1216–1229. doi:doi:10.1016/j.ress.2010.06.015.

[15] S. Touzani, D. Busby, Smoothing spline analysis of variance approach for global sensitivity analysis of computer codes, Reliability Engineering and System Safety 112 (2013) 67–81. doi:doi:10.1016/j.ress.2012.11.008.

[16] M. Ratto, A. Pagano, P. Young, State dependent parameter metamodelling and sensitivity analysis, Computer Physics Communications 177 (11) (2007) 863–876. doi:doi:10.1016/j.cpc.2007.07.011.

[17] M. Ratto, A. Pagano, Using recursive algorithms for the efficient identification of smoothing spline ANOVA models, AStA Advances in Statistical Analysis 94 (4) (2010) 367–388. doi:10.1007/s10182-010-0148-8.

[18] E. Borgonovo, W. Castaings, S. Tarantola, Model emulation and moment-independent sensitivity analysis: an application to environmental modelling, Environmental Modelling & Software 34 (2012) 105–115. doi:doi:10.1016/j.envsoft.2011.06.006.

[19] J. E. Oakley, A. O'Hagan, Probabilistic sensitivity analysis of complex models: a Bayesian approach, Journal of the Royal Statistical Society: Series B (Statistical Methodology) 66 (3) (2004) 751–769. doi:10.1111/j.1467-9868.2004.05304.x.

[20] J. P. Kleijnen, Kriging metamodeling in simulation: a review, European Journal of Operational Research 192 (3) (2009) 707–716. doi:doi:10.1016/j.ejor.2007.10.013.

[21] W. Kik, J. Piotrowski, A fast, approximate method to calculate normal load at contact between wheel and rail and creep forces during rolling, in: Proceedings of the 2nd Mini Conference on Contact Mechanics and Wear of Rail/Wheel Systems, 1996.

[22] P. Bolton, P. Clayton, Rolling-sliding wear damage in rail and tyre steels, Wear 93 (2) (1984) 145–165. doi:10.1016/0043-1648(84)90066-8.

[23] N. Cressie, Statistics for spatial data, Revised Edition, Wiley, 1993.

[24] R. Johnson, D. Wichern, Applied Multivariate Statistical Analysis, 6th Edition, Pearson, 2007.

[25] J. Sikorska, M. Hodkiewicz, L. Ma, Prognostic modelling options for remaining useful life estimation by industry, Mechanical Systems and Signal Processing 25 (5) (2011) 1803–1836. doi:10.1016/j.ymssp.2010.11.018.

[26] J. Lee, F. Wu, W. Zhao, M. Ghaffari, L. Liao, S. D., Prognostics and health management design for rotary machinery systems reviews, methodology and applications, Mechanical Systems and Signal Processing 42 (1-2) (2014) 314–334. doi:10.1016/j.ymssp.2013.06.004.

[27] P. Baraldi, F. Cadini, F. Mangili, E. Zio, Model-based and data-driven prognostics under different available information, Probabilistic Engineering Mechanics 32 (2013) 66–79. doi:10.1016/j.probengmech.2013.01.003.

[28] Y. Hu, P. Baraldi, F. Di Maio, E. Zio, A particle filtering and kernel smoothing-based approach for new design component prognostics, Reliability Engineering and System Safety 134 (2015) 19–31. doi:10.1016/j.ress.2014.10.003.

[29] F. Braghin, S. Bruni, R. F., Wear of railway wheel profiles: a comparison between experimental results and a mathematical model, Vehicle System Dynamics Supplement 37 (2002) 478–489.
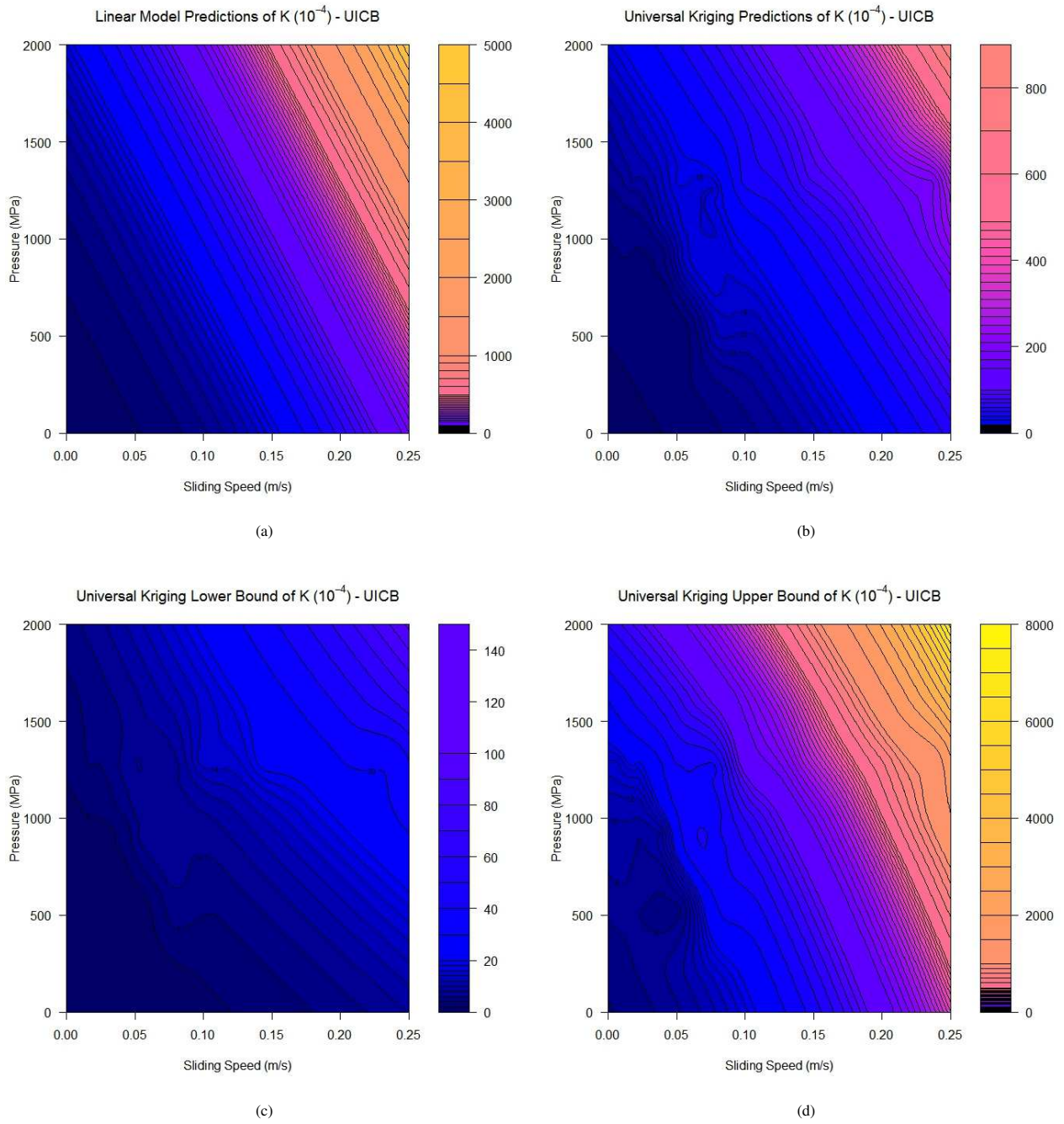
AppendixA. Additional figures

Figure A.11: Wear coefficient K (10^{-4}) maps concerning UICB rail discs: (a) describes the drift given by the linear model (large scale variability); (b) is the prediction with universal kriging; (c) and (d) show the 90% pointwise prediction intervals.
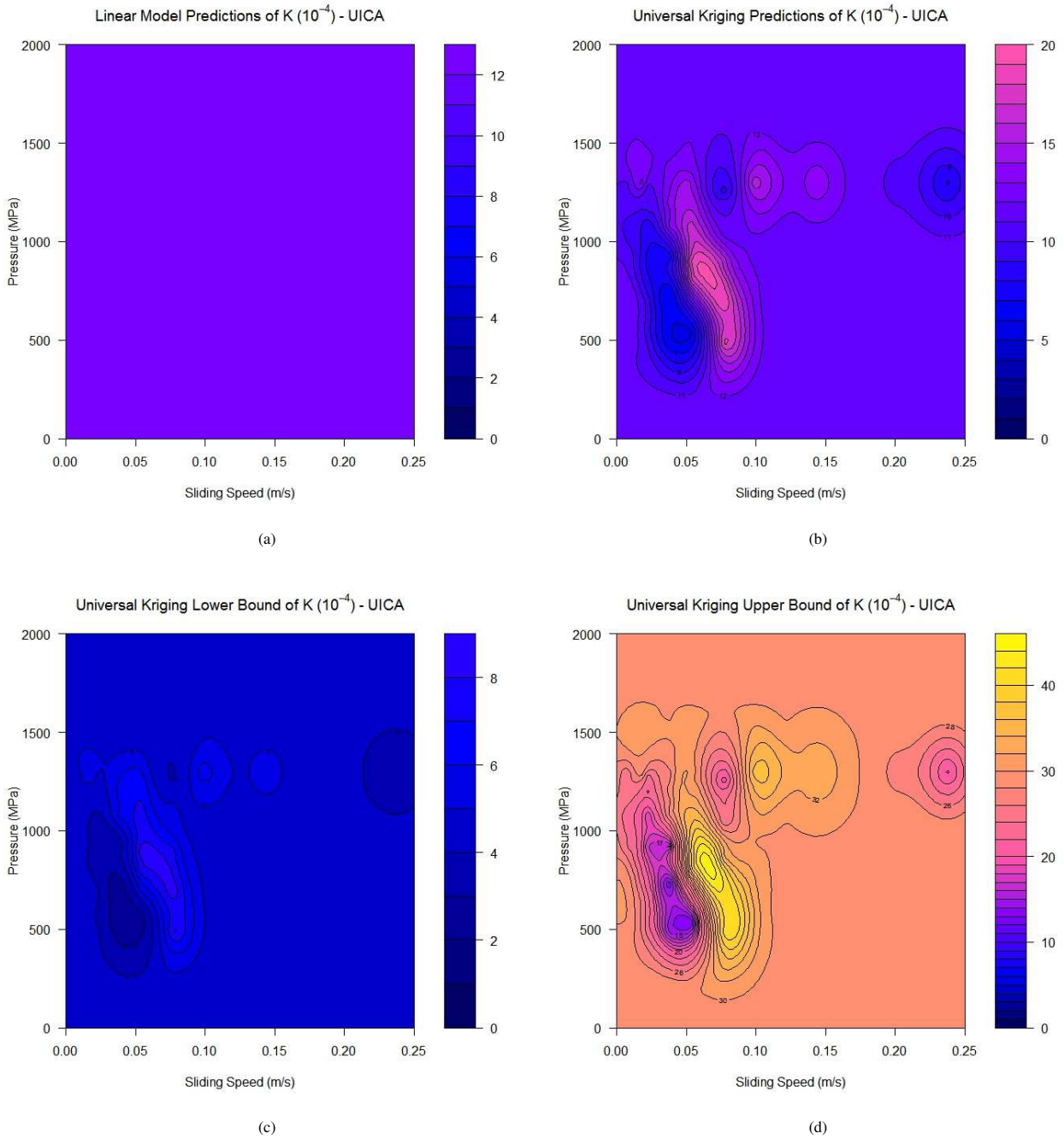
Figure A.12: Wear coefficient K (10^{-4}) maps concerning UICA rail discs: (a) describes the drift given by the linear model (large scale variability); (b) is the prediction with universal kriging; (c) and (d) show the 90% pointwise prediction intervals.
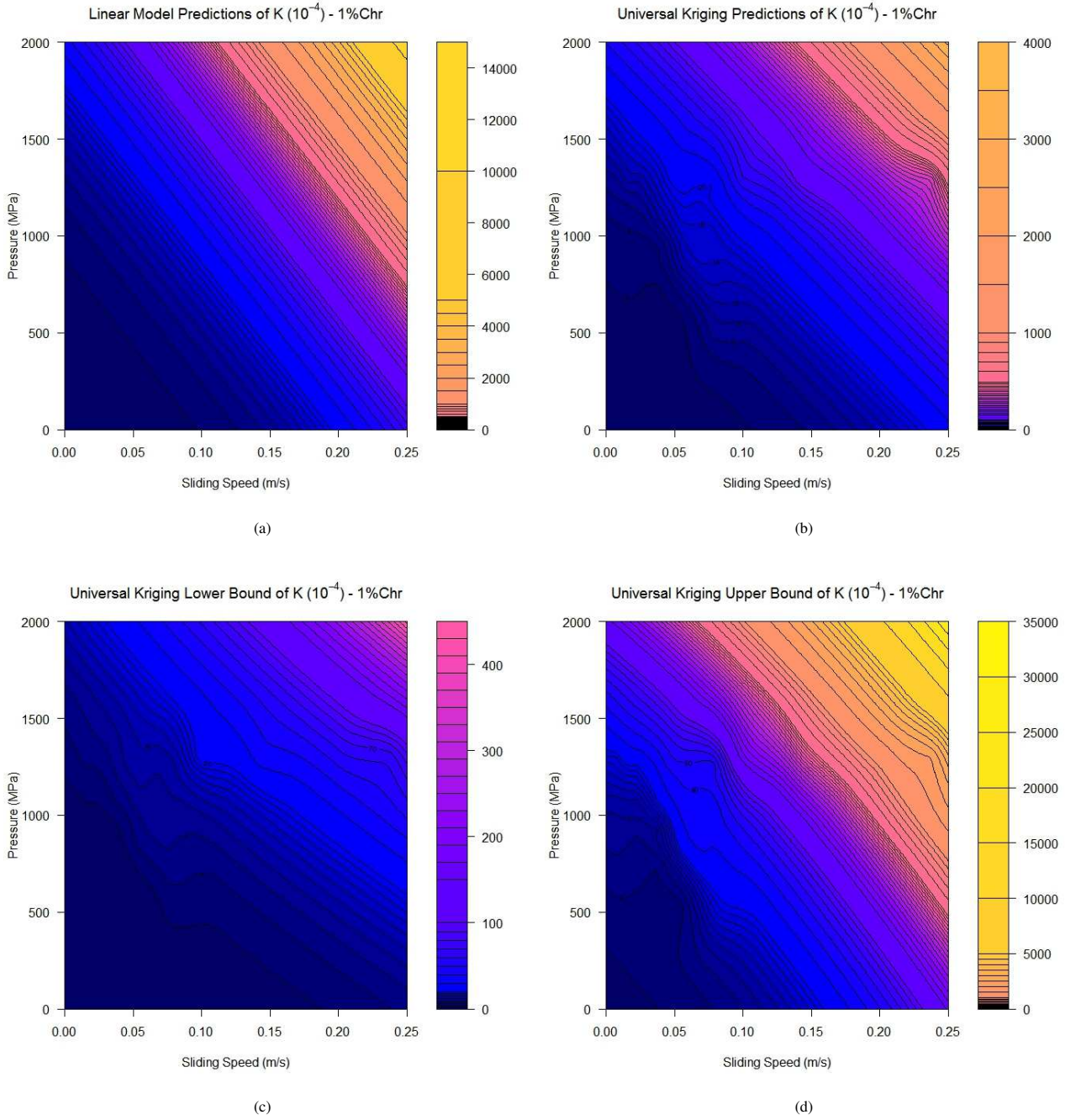
Figure A.13: Wear coefficient *K* (10^{-4}) maps concerning 1%Chr rail discs: (a) describes the drift given by the linear model (large scale variability); (b) is the prediction with universal kriging; (c) and (d) show the 90% pointwise prediction intervals.